

# UNCLASSIFIED

AD NUMBER
AD848309
NEW LIMITATION CHANGE
TO Approved for public release, distribution unlimited
FROM Distribution authorized to U.S. Gov't. agencies only; Administrative/Operational Use; JAN 1969. Other requests shall be referred to Naval Civil Engineering Lab., Port Hueneme, CA 93041.
AUTHORITY
NCEL ltr, 17 Sep 1979

THIS PAGE IS UNCLASSIFIED

4  
AD848309

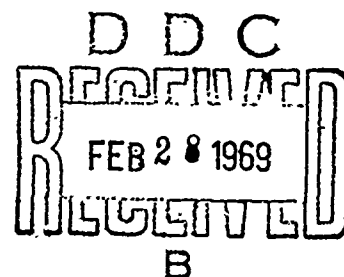
Technical Note N-1005

A POTENTIOSTATIC DEZINCIFICATION STUDY

By

Howard A. Porte

January 1969



Each transmittal of this document outside the agencies of the U. S. Government must have prior approval of the U. S. Naval Civil Engineering Laboratory.

NAVAL CIVIL ENGINEERING LABORATORY  
Port Hueneme, California 93041

# A POTENTIOSTATIC DEZINCIFICATION STUDY

Technical Note N-1005

Y-F015-20-02-024

by

Howard A. Porte

## ABSTRACT

The objective of this study was to determine the dezincification rate of commercially available valve stems containing varying amounts of zinc. Potentiostatic anodic polarization tests were conducted on copper (electrolytic tough pitch) and four copper alloys - copper alloy 377 (forging brass), ASTM B140 Alloy "A" (lead red brass), ASTM B62 (85-5-5-5), and copper alloy 624 (aluminum bronze) - in laboratory tap water at 25C (77F) and 50C (122F) and in 0.5 molar aqueous sodium chloride (0.5M NaCl) at 25C. Dezincification was found in copper alloy 377 in laboratory tap water at 25C, corroborating field experience that high zinc content valve stems are subject to dezincification attack. Both ASTM B140 Alloy "A" and copper alloy 624 showed no visible attack at 25C in laboratory tap water but did show evidence of dealloying attack at 50C; these alloys could be expected to perform satisfactorily in cold water but are not recommended for hot water systems. ASTM B62 did not show any dezincification attack at 50C in laboratory tap water, this alloy is recommended for valve stems in both cold and hot water systems. These tests suggest that the potentiostatic method is applicable as an accelerated test for detecting susceptibility to dealloying attack in copper alloys.

Each transmittal of this document outside the agencies of the U. S. Government must have prior approval of the U. S. Naval Civil Engineering Laboratory.	
34	35
DISTRIBUTION/AVAILABILITY CODES	WRITE SECTION
DIST.	UNCLASSIFIED
AVAIL.	CONFIDENTIAL
AND/OR SPECIAL	SECRET
	<input type="checkbox"/> <input type="checkbox"/> <input type="checkbox"/>

## INTRODUCTION

One of the reasons that copper is widely used in fresh water and sea water systems is because it has good corrosion resistance. In some applications where high strength is required, such as water valve stems, brasses or bronzes are usually employed. When these copper alloys are used it is generally hoped that their corrosion resistance will be similar to that of copper. However, some copper-zinc alloys in some environments are subject to a type of corrosion known as dezincification in which zinc corrodes preferentially, leaving a porous residue of copper and corrosion products and reducing the tensile strength and ductility of the alloy. When this occurs, valve stem failure results, often necessitating complete valve replacement at considerable cost. Dezincification in manganese bronze (58% copper, 33% zinc) valve stems has been experienced in the Los Angeles, California water system as reported by Tabor.<sup>1</sup> Extensive valve system failures, attributed to dezincification, have also occurred at the San Diego, California, Naval Hospital and other stations within the Eleventh Naval District.

The environmental conditions which favor dezincification are (1) high temperature, (2) poor aeration or stagnant conditions, (3) acid or alkaline water, (4) high chloride ion content, (5) soft water containing fresh carbon dioxide. The general consensus of corrosion authorities is that copper-zinc alloys containing more than 15% zinc are susceptible to this type of attack and that the susceptibility increases with increasing zinc content; according to Uhlig,<sup>2</sup> "brasses which contain 15% or less of zinc are usually immune." However, there is no theoretical explanation for this immunity below 15%, if indeed it be so. Upon Tabor's recommendation the Department of Water and Power, Los Angeles and the Water Department, San Diego began to specify stem materials with a 7% maximum zinc content. In 1963, Southwest Division, Naval Facilities Engineering Command, wrote a new valve specification with a similar 7% zinc content maximum for valve stems. A later paper by Palmer<sup>3</sup> of Anaconda American Brass Company, disputed the 7% specification as being too severe and presented evidence that dezincification was not observed with Colorado river water in copper alloy #220 (Cu 90.7%, Zn 9.3%) or copper alloy #6941 (Cu 81.7, Zn 14.6, Si 3.5, and Fe 0.2%).

The ultimate test of whether or not an alloy is susceptible to dezincification would be the results obtained under actual service conditions. However, in some cases it might take months or even years before dezincification developed. It was the objective of this investigation to determine the dezincification rate of commercially available

valve stems containing varying amounts of zinc in softened and chlorinated Colorado river water. The approach was to determine the relative susceptibility to dezincification of the valve stem alloys after accelerated corrosion attack caused by anodic potentiostatic polarization.

## EXPERIMENTAL

The materials used in this study were: copper 110 (electrolytic tough pitch copper), copper alloy 377 (forging brass), ASTM B140 Alloy "A" (lead red brass), ASTM B62 (85-5-5-5), and copper alloy 624 (aluminum bronze); ASTM B140 Alloy "A" and ASTM B62 were obtained from the valve stems of commercially available valves and the other materials were procured in the form of  $\frac{1}{2}$ " round rod. The chemical composition of the materials are given in Table 1.

Small cylindrical electrodes were sectioned from the rod material, ground and polished using up through 600 grit silicon carbide paper, and placed in a specially constructed Teflon electrode holder so that only one surface, in the form of a disk approximately 1.25 cm<sup>2</sup> in area, was exposed to the solution. During the experiments the electrode was rotated at a speed of 100rpm.

The electrochemical polarization was performed with an electronic potentiostat, Wenking Model 61-TR, in a conventional three electrode cell; platinum was used as the auxiliary electrode and saturated calomel as the reference electrode. Potential sweep rates of 4 volts/hr were generated by feeding the output from an Erwin Halstrup model MP64 motor potentiometer into the potentiostat. Potentials were measured with a Keithley Model 61CB Electrometer with an input impedance of  $10^{14}$  ohms. Current was measured by determining the voltage drop across a precision 1 ohm resistor and amplifying with a DANA model 3850 DC amplifier. Current and potential were recorded simultaneously on (1) a Leeds and Northrup Speedomax G 2-pen recorder and (2) an Ampex Series 800B tape recorder. The polarization curves (Figures 1 to 10) were obtained by converting the data on magnetic tape to punched cards via an analog-to-digital converter and an IBM 1620 II computer; a special Fortran II program and an IBM 1627 plotter then produced the curves.

Polarization experiments were conducted under air-saturated or nitrogen-saturated conditions in the following solutions: (1) Laboratory tap water at temperatures of 25 and 50C and, (2) 0.5 molar aqueous sodium chloride (0.5 M NaCl) at 25C. The 0.5M NaCl aqueous solution was selected because dezincification is accelerated by chloride ions.

The Laboratory water is obtained from wells and then chlorinated and softened to a total hardness (as CaCO<sub>3</sub>) of approximately 5 grains/gal. (85 ppm); the chloride ion concentration in the water, measured before softening, is approximately 50 ppm and total dissolved solids averaged about 1000 ppm.

The polarization cell was a 1-liter beaker with an acrylic plastic top containing five portholes through which the working electrode, reference electrode, counter electrode, gas-inlet tube and thermometer were inserted.

For deaerated experiments nitrogen was bubbled through the solution for at least 16 hours before inserting the electrode assembly and the nitrogen flow was continued throughout the experiment; for aerated experiments, air was bubbled through the solution for at least 1 hour.

The polarization cell was immersed in a constant temperature bath so that temperature variation was less than  $\pm 1^\circ\text{C}$ . Unless otherwise specified, the working electrode was rotated at 100 rpm. Pretreatment of the working electrode consisted of a cathodic polarization from the corrosion potential to ca. -1000 mv vs. S.C.E. The electrode was then allowed to come to the steady-state corrosion potential before anodic polarization was started.

## RESULTS.

Anodic potentiostatic polarization curves of copper 110, (electrolytic tough pitch), ASTM B140 Alloy "A" (lead red brass), ASTM B62 (85-5-5-5), copper alloy 377 (forging brass) and copper alloy 624 (aluminum bronze) in 0.5 M aqueous NaCl and NCEL tap water are shown in Figures 1-10. A summary of important polarization characteristics is shown in Table 2. The relative corrosion rates are given in column

$$\frac{\Delta I}{\Delta E}$$

The corrosion rate is obtained from the "polarization resistance" which is defined by the equation

$$\frac{\Delta E}{\Delta I} = \frac{B_a B_c}{2.3 I_{\text{corr}} (B_a + B_c)}$$

where  $\Delta E/\Delta I$  is the polarization resistance,  $B_a$  and  $B_c$  are the slopes of the local cathodic and anodic curves, and  $I_{\text{corr}}$  is the corrosion current.  $\Delta E$  is the polarized potential within 10 to 15 millivolts of the corrosion potential and  $\Delta I$  is the corresponding polarizing current; these values are obtained directly from computerized print-outs of the polarization data. Taking the anodic and cathodic slopes as constants, the equation may be rearranged to give  $I_{\text{corr}} = k \Delta I / \Delta E$ , showing that the open-circuit corrosion rate is proportional to the inverse polarization resistance.

\*See Appendix A

The amount of anodic attack on a specimen was assessed from the polarization curve supplemented by visual inspection. The presence (or absence) of dezincification or dealuminization in the alloys was determined primarily by visual inspection and observation of specimens in an optical microscope. Those specimens which had a reddish colored surface after polarization were considered to have undergone some dealloying. Because of the extreme thinness of the surface layer it was not possible to confirm this conclusion by metallurgical analysis in most cases. For two specimens that were subjected to metallurgical analyses, one forging brass and one aluminum bronze, dezincification was confirmed in the forging brass but dealuminization could not be detected in the aluminum bronze. The polarization curves for copper, forging brass, and aluminum bronze in deaerated 0.5M NaCl are illustrated in Figure 1; the polarization curves for copper and aluminum bronze in aerated 0.5M NaCl are illustrated in Figure 2. In both aerated and deaerated 0.5M NaCl the primary passive potential ( $E_{pp}$ )\*\* for all materials was in the region +20 to +100 mv. versus S.C.E. The critical anodic current density,  $I_{cr}$  was approximately  $17,000 \text{ uA/cm}^2$  for copper compared to approximately  $28,000 \text{ uA/cm}^2$  for both forging brass and aluminum bronze. The relative corrosion rates ( $\Delta I/\Delta E$ ) for all materials were low in deaerated 0.5M NaCl; in aerated solution the corrosion rate for copper was found to be about twice as great as that for aluminum bronze. Corrosion potentials ( $E_{corr}$ ) were somewhat more noble (more positive) in aerated 0.5M NaCl. Copper showed uniform attack over the entire surface. Visual inspection indicated dezincification in the forging brass and this was confirmed by metallurgical examination of one of the forging brass specimens. Visual inspection indicated dealuminization of the aluminum bronze but this could not be verified by metallurgical analysis probably because the corroded layer was too thin.

The electrochemical behavior of aluminum bronze and forging brass in nitrogen saturated tap water at 25C is illustrated in Figure 3. Although no  $E_{pp}$  is exhibited it can be seen that for the brass specimens the current rises very sharply in the potential region -40 to +100 millivolts. For aluminum bronze the current also begins to rise in this potential region but not steeply as the forging brass and the current is significantly below that of forging brass at more noble potentials. The open-circuit corrosion rate of both alloys was very low. After the anodic polarization runs the forging brass showed definite signs of attack as evidenced by the reddish-orange colored surface whereas the aluminum bronze did not show any visible attack and no discoloration of the surface was apparent.

A polarization experiment was performed with the forging brass electrode held stationary instead of being rotated at 100 rpm as was

\*\*See Appendix A.

done in all other experiments. As shown in Figure 4, the current rise begins at approximately the same potential but rises in a much more gradual manner than was the case for the rotated electrode.

The polarization behavior of aluminum bronze and forging brass in air saturated tap water at 25C is illustrated in Figure 5. The general shape of these curves is the same as in the nitrogen saturated solution, although the current densities are slightly higher for both alloys. The relative corrosion rates, that is the inverse "polarization resistance" values, listed in Table 2 are higher in the case of air saturated tap water, 0.5 for forging brass and 0.2 for aluminum bronze as compared to 0.1 for both alloys in deaerated tap water. In addition to its higher corrosion rates the forging brass also showed evidence of corrosion attack by virtue of the bright orange-red surface after polarization. The aluminum bronze in contrast showed no visible attack in the aerated solution after polarization.

The effect of temperature was examined by performing polarization experiments at 50C in tap water. The results for aluminum bronze and forging brass in nitrogen saturated tap water are shown in Figure 6. As was the situation at 25C the current rise for the forging brass is again steeper than that of the aluminum bronze in the potential range 0 to 100 millivolts. The forging brass again appeared to be extensively attacked as evidenced by the orange-red color surface after polarization. The aluminum bronze which showed no attack at 25C showed some slight attack around the outer edge of the specimen at 50C.

In aerated tap water at 50C the aluminum bronze showed essentially the same polarization curve as in deaerated solution at 50C (Figure 7). The open-circuit corrosion rates for aluminum bronze in both aerated and deaerated solution were low at 50C as was the corrosion rate for forging brass in deaerated solution at 50C.

The polarization curves for two commercially available valve stem materials - ASTM B140 Alloy "A", an intermediate (11 to 15%) zinc content alloy and ASTM B62, a low (4 to 6%) zinc content alloy - in aerated laboratory tap water are shown in Figures 8 to 10. ASTM B140 Alloy "A" showed negligible corrosion attack at 25C; however, at 50C definite corrosion attack and probable dezincification was indicated by a copper layer deposited on the surface. The polarization curves for ASTM B140 Alloy "A" at 25C and 50C in Figures 8 and 9 are very similar in spite of the observable difference in corrosion attack at the two temperatures. Figure 10 shows the polarization curve for ASTM B62 in aerated tap water at 50C. The curve has the same general shape as ASTM B140 Alloy "A" but exhibits somewhat lower current densities in the more noble potential region. Visual inspection of the surface showed negligible dezincification attack demonstrating the superior corrosion resistance of this alloy compared to the other alloys studied in this investigation.



## DISCUSSION

There are two mechanisms commonly advanced to explain the dealloying phenomenon.<sup>4</sup> (For copper-zinc alloys this is referred to as dezincification, for copper-aluminum alloys this referred to as dealuminization.) As applied to dezincification: In mechanism (1) zinc is supposed to dissolve selectively leaving a porous residue of copper; in mechanism (2) both metals are supposed to dissolve simultaneously followed by the subsequent redeposition of copper. Experimental data has been recorded supporting both mechanisms;<sup>5,6</sup> however, no conclusive evidence substantiating one or the other has been demonstrated.

In this investigation it was found that both copper alloys-CA377, forging brass and CA 624, aluminum bronze-showed higher critical anodic current densities,  $I_{cr}$  than did pure copper in 0.5 M NaCl. The value of  $I_{cr}$  was essentially the same for both forging brass and aluminum bronze. The outward appearance of both specimens showed about the same amount of attack; however, metallurgical examination revealed that the forging brass had undergone some dezincification but similar examination of the aluminum bronze did not confirm dealuminization. Repeat polarization of these specimens did not significantly change the shape of the polarization curve and  $E_{pp}$  and  $I_{cr}$  had essentially the same values on the second or third polarization curves as on the first. Interpreting these results for the forging brass in terms of the two mechanisms proposed for dezincification, if the selective removal of zinc mechanism were operating then as dezincification progressed the brass structure would become depleted in zinc and it would be expected that each succeeding polarization curve should show decreasing values of  $I_{cr}$  and tend to approach the curve of pure copper. The appearance of the forging brass surface changed considerably after only one anodic polarization, apparently due to the build up of copper on the surface. But since the shape of the polarization curves did not change on the second or even the third polarization on the same specimen this indicated that the surface being anodically oxidized during the polarization was the same. This means that the matrix of the alloy does not change during the subsequent polarizations thus lending support to the redeposition of copper mechanism. It should be emphasized at this point that an anodic polarization scan, of less than 15 minutes duration, produces relatively little corrosion and in fact a specimen of forging brass which was metallographically examined after three anodic polarizations in 0.5 M NaCl showed only a small amount of dezincification and a small amount of overall corrosion even though the color of the surface was completely changed from the initial gold color to a reddish-orange color. An experiment which is suggested, but which has not been tried in the present investigation, would be to anodically polarize a specimen for an extended period of time to produce extensive corrosion, and presumably a great deal of dezincification, and then obtain a second polarization curve on this extensively corroded specimen.

If the polarization curve again were identical to the original polarization curve this would be conclusive evidence that the matrix was unchanged after extensive dezincification. An experiment which was tried was the polarization of a forging brass specimen where the electrode was held stationary in tap water (Figure 4). In this situation the corrosion products would be expected to remain in the vicinity of the corroding specimen for a longer period of time than would be the case where rotation occurred and more rapid diffusion into the bulk solution could take place. The result was that for the stationary electrode the current rise was much more gradual than for the rotating electrode. The more slowly rising current could be interpreted as due to the corrosion products being protective, thus causing a lower current, as would be the case after  $I_{cr}$  is reached, where the current decreased again after a protective oxide was deposited on the surface.

The corrosion rate was found to be low for all materials in nitrogen saturated solutions as would be expected. In air saturated 0.5M NaCl the indicated corrosion rate of pure copper was about twice as fast as for aluminum bronze. In air saturated tap water at 25C forging brass was found to corrode about twice as fast as aluminum bronze. These results are consistent with the work reported by Southwell<sup>7</sup> in which aluminum bronze was found to exhibit superior corrosion resistance compared to copper and zinc content copper alloys submerged in tropical sea water and fresh water for 15 years. Both aluminum bronze and forging brass showed increased corrosion in the chloride solution compared to tap water. The aluminum bronze was adversely affected by the increase from 25C to 50C in tap water. This was shown in the polarization curves (Figure 6 compared to Figure 3) where aluminum bronze showed definitely increased corrosion currents at 50C and in the appearance of the specimens, since at 50C definite attack was seen along the outer edge of the specimen whereas at 25C no visible sign of attack was observed. The forging brass exhibited high corrosion currents in the polarization curves and large amount of visible attack at both temperatures. As is shown in Figure 6 at 50C in the potential range +50 to +400 mv., aluminum bronze exhibited lower currents than did forging brass; however, at more noble potentials, more than 400 millivolts, forging brass actually showed lower corrosion currents than aluminum bronze.

The corrosion behavior of ASTM B140 Alloy "A" also was adversely affected by the temperature increase from 25C (77F) to 50C (122F) although the polarization curves were essentially the same at both temperatures. ASTM B62 was the only alloy not attacked at 50C in aerated tap water.

A significant result of this study is that it demonstrates how potentiostatic polarization measurements can be utilized in predicting the susceptibility of copper alloys to dezincification in real environments.

### Cost Consideration

When valve stem failure occurs it is often necessary to replace the entire valve. Therefore in areas where dezincification is known to be a problem, it may be more economical to use a valve with a low zinc content valve stem even if the initial cost of this valve is higher than a comparable valve with a higher zinc content valve stem. As an example, consider three bronze globe valves, class 100#, size 1", offered by a major valve company:

<u>Valve</u>	<u>Valve Stem</u>	<u>Cost</u>
1	ASTM B140 Alloy A <sup>2/</sup>	\$8.60
2	ASTM B99 Alloy B <sup>1/</sup>	9.40
3	ASTM B99 Alloy B <sup>1/</sup>	12.60

<sup>1/</sup>ASTM B99 Alloy B; zinc content 1.5%

<sup>2/</sup>ASTM B140 Alloy A; zinc content 11 to 15%

The initial cost of valve 1 is lowest but it contains the highest zinc-content valve stem and, therefore, it probably would suffer dezincification attack and require replacement before either valve 2 or valve 3 would. In order to determine the most economical choice it is necessary to perform a present valve analysis for the three valves; this analysis is presented in Appendix C.

### CONCLUSIONS AND RECOMMENDATIONS

1. Potentiostatic anodic polarization rapidly produced dezincification in copper alloy 377 (forging brass) - a high zinc content (34% zinc) copper alloy - in laboratory tap water and 0.5 molar aqueous sodium chloride at 25C, corroborating field experience that high zinc content alloys are subject to dezincification attack; high zinc content copper alloys are not recommended for valve stems in softened or high chloride waters.

2. Copper alloy 624 (aluminum bronze) showed better corrosion resistance than copper alloy 377 by virtue of lower relative corrosion rate, lower anodic current densities and less visible attack in laboratory tap water at 25C but did show some dealuminization at 50C (122F) in laboratory tap water and in 0.5M NaCl at 25C; copper-aluminum alloys are not recommended for valve stems in warm softened water or high chloride waters.

3. ASTM B140 Alloy "A" (11 to 15% zinc) showed good corrosion resistance at 25C in aerated laboratory tap water but exhibited some

dezincification at 50C; this alloy could be expected to perform satisfactorily in low chloride, cold water systems but is not recommended for hot water or high chloride water.

4. ASTM B62 (4 to 6% zinc) showed good corrosion resistance in aerated tap water at 50C (122F) and in accordance with a present value analysis (Appendix C) ASTM B62 or a similar low zinc content alloy is recommended for use in both cold and hot water systems.

5. Dealloying and corrosion rates are increased at elevated temperatures and in high chloride waters.

6. Potentiostatic anodic polarization, in conjunction with visual inspection and metallurgical examination, can quickly give information concerning the propensity of copper alloys to dealloying attack; the potentiostatic method is recommended as an accelerated test for detecting the susceptibility of copper-zinc alloys to dezincification.

#### ACKNOWLEDGEMENT

Mr. Fred Reinhart made the metallurgical analysis and interpreted the findings of these analysis. The assistance of Mr. Charles W. Mathews in performing the polarization experiments is acknowledged. The assistance of Mr. Arlyn Jackson in the data reduction of the data from magnetic tapes is acknowledged.

Table 1. Chemical Composition of Copper Alloys

Alloy	Element (%)					
	Cu	Zn	Al	Pb	Fe	Sn
Copper 110 (copper)	99.9					
Copper Alloy 377 (forging brass)	61.6	34.2		2.1		
Copper Alloy 624 (aluminum bronze)	84.9	<.05	10.7		3.5	
ASTM B140 Alloy "A" (leaded red brass)	83.5 to 86.5	Rem.		1.5 to 2.2	0.1	
ASTM B62 (85-5-5-5)	84.0 to 86.0	4 to 6		4 to 6	0.3	4 to 6

Table 2. Potentiostatic Anodic Polarization Characteristics.

Material	Polar. Curve Figure	Experimental Conditions		$E_{corr}$ mv vs. S.C.E. Corrosion Potential	$\Delta I/\Delta E$ $\mu A/mv$ Relative Corrosion Rate at $E_{corr}$	$E_{pp}$ mv vs. S.C.E. Primary Passive Potential	$I_{cr}$ $\mu A/cm^2$ Critical Current	Type of Corrosion Attack <sup>2</sup>
		Solution	Temp. °C					
Copper 110	1	(N)0.5N NaCl	25	-296	0.2	+22	17,570	U
	2	(A)0.5N NaCl	25	-216	3.5	+88	15,700	U
Copper Alloy No. 377	1	(N)0.5N NaCl	25	-259	0.2	+54	27,760	DZ <sup>3</sup>
	3	(N) TW	25	-152	0.1			DZ
	5	(A) TW	25	-123	0.5			DZ
	6	(N) TW	50	-204	0.2			DZ
	4	(N) TW (S)	25	-153	0.1			DZ
	1	(N)0.5N NaCl	25	-278	0.3	+106	28,140	DA
Copper Alloy No. 624	2	(A)0.5N NaCl	25	-253	1.7	+97	26,990	DA
	3	(N) TW	25	-235	0.1			N
	5	(A) TW	25	-79	0.2			N
	6	(N) TW	50	-200	0.2			LDA
	7	(A) TW	50	-63	0.2			LDA
	8	(A) TW	25	-80	0.1			N
ASTM B140 Alloy "A"	9	(A) TW	50	-77	0.3			LDZ
	10	(A) TW	50	-100	0.2			N

1. (N)=Nitrogen saturated, (A)=Air saturated, TW=Tap water, Electrode rotated at 100 rpm in all experiments except those designated (S)=Stationary.
2. Type of Corrosion Attack as Determined by Visual Inspection: U=Uniform attack; DZ=Dezincification; DA=Dealuminization; LDA=Small amount of attack, Dealuminization; LDZ=Small amount of attack, Dezincification; N=Negligible attack.
3. Metallurgical examination of this specimen showed dezincification.

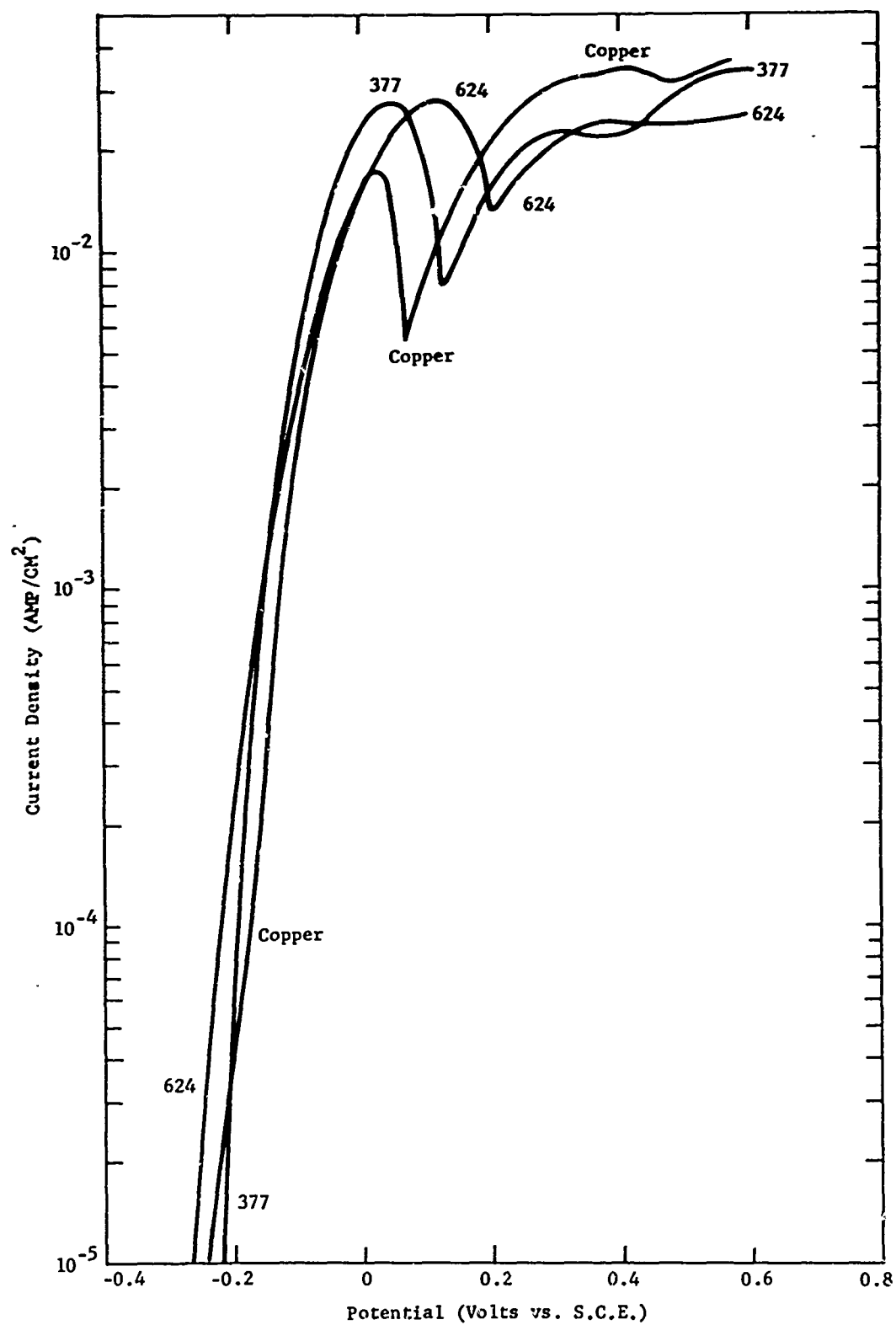


Figure 1. Anodic polarization of copper, copper alloy 624 and copper alloy 377 in nitrogen-saturated 0.5M NaCl at 25C.

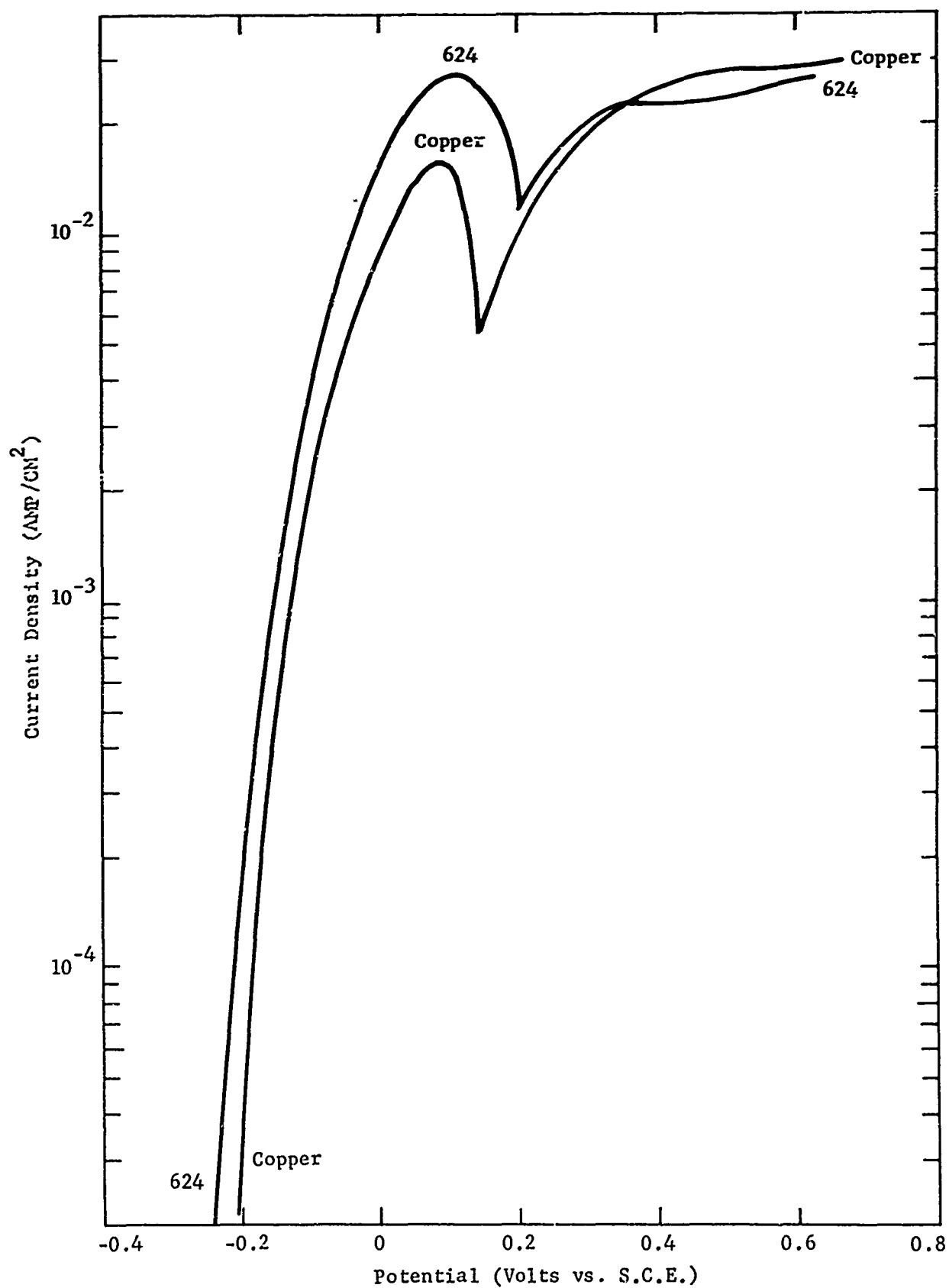


Figure 2. Anodic polarization of copper and copper alloy 624 in air-saturated 0.5M NaCl at 25C.



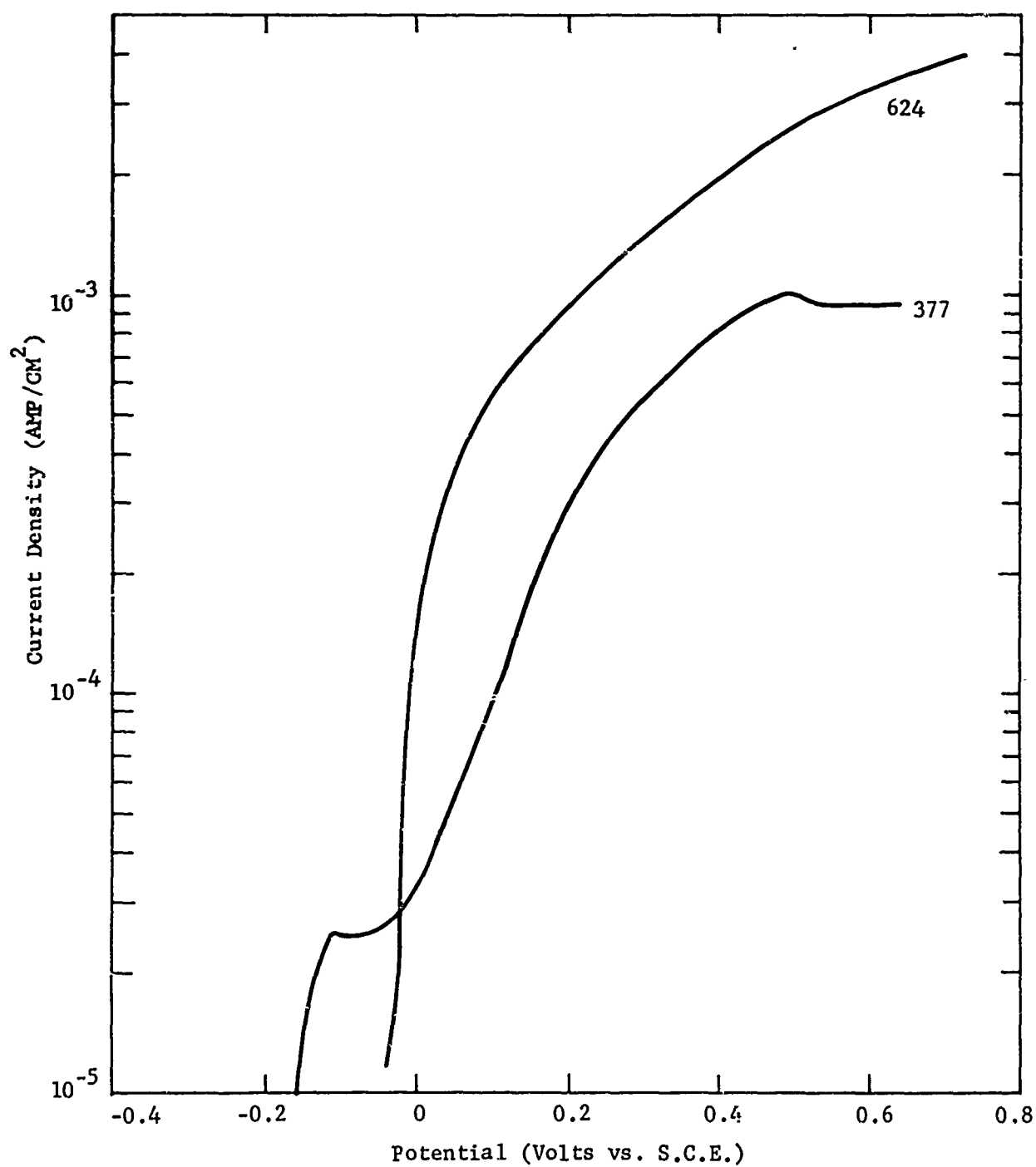


Figure 3. Anodic polarization of copper alloy 624 and copper alloy 377 in nitrogen-saturated tap water at 25C.

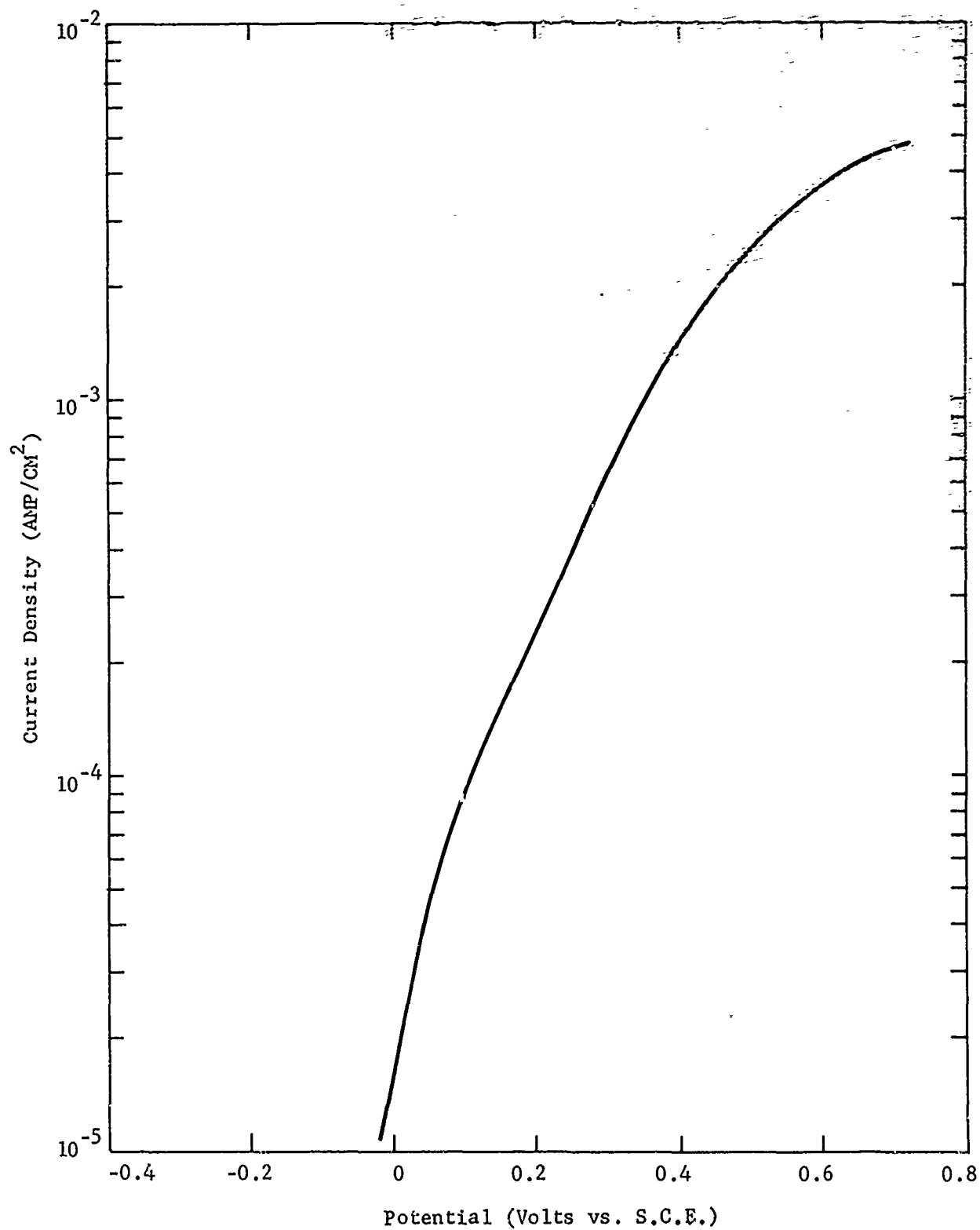


Figure 4. Anodic polarization of copper alloy 377 in nitrogen-saturated tap water at 25C. Stationary electrode.

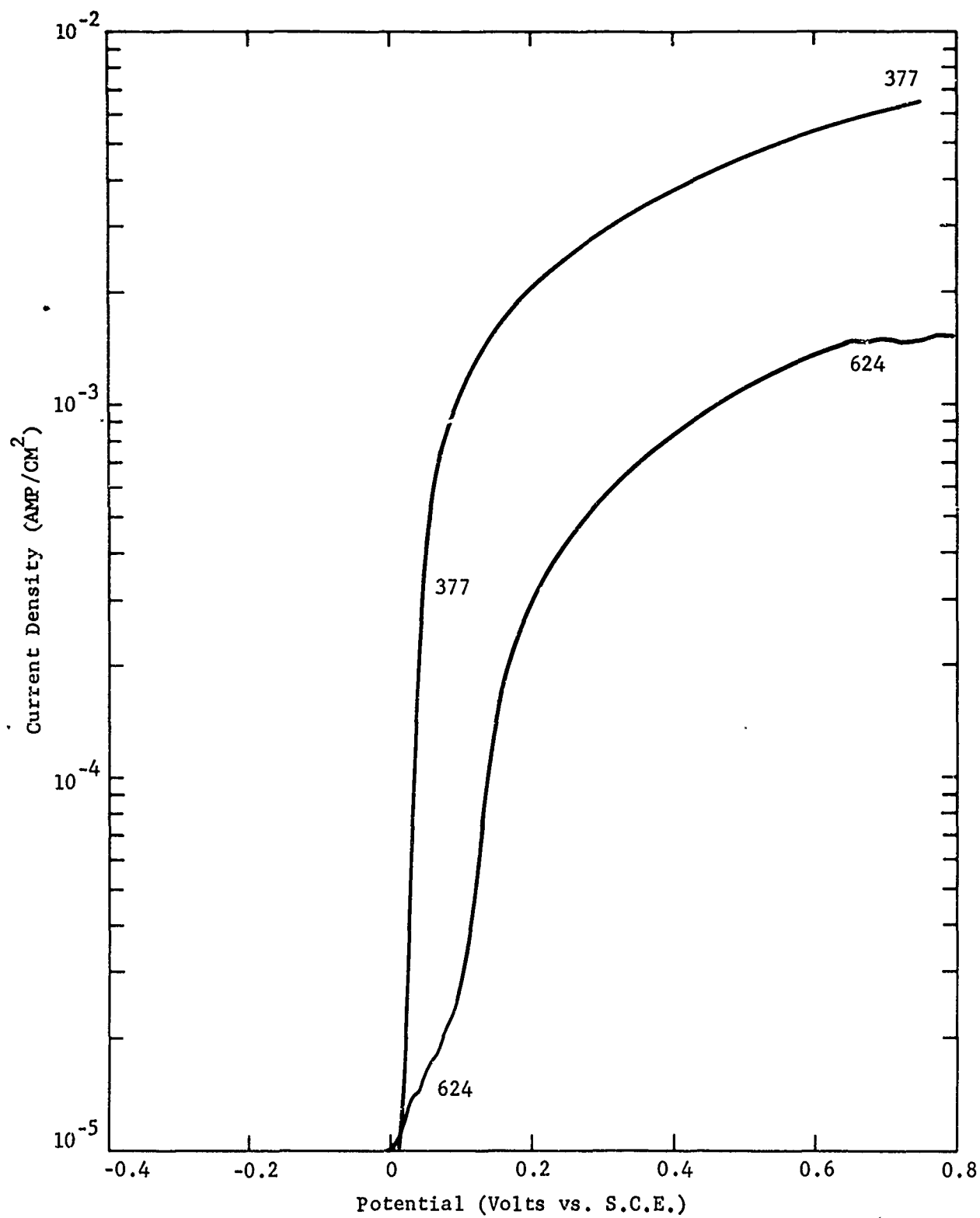


Figure 5. Anodic polarization of copper alloy 624 and copper alloy 377 in air-saturated tap water at 25C.

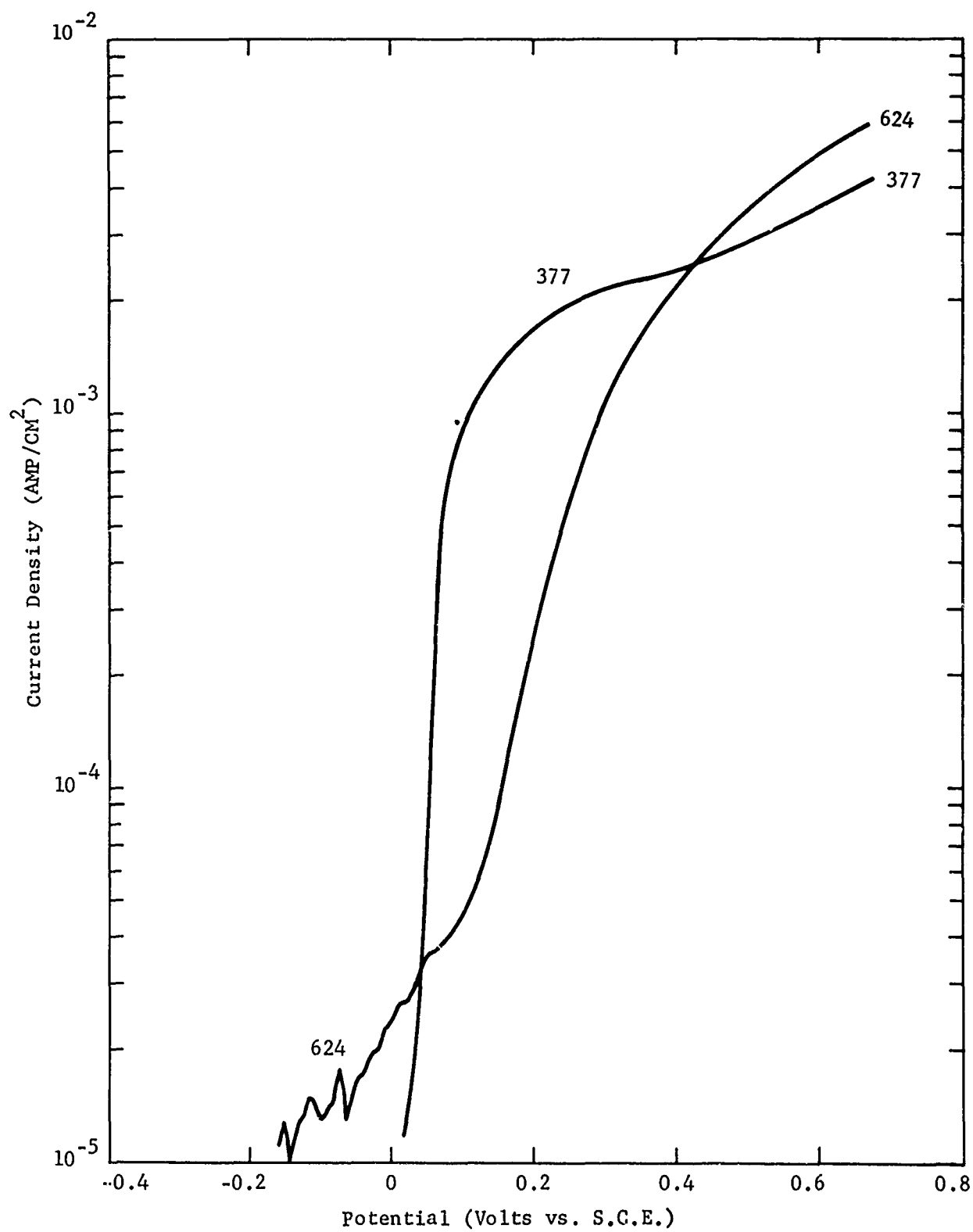


Figure 6. Anodic polarization of copper alloy 624 and copper alloy 377 in nitrogen-saturated tap water at 50C.

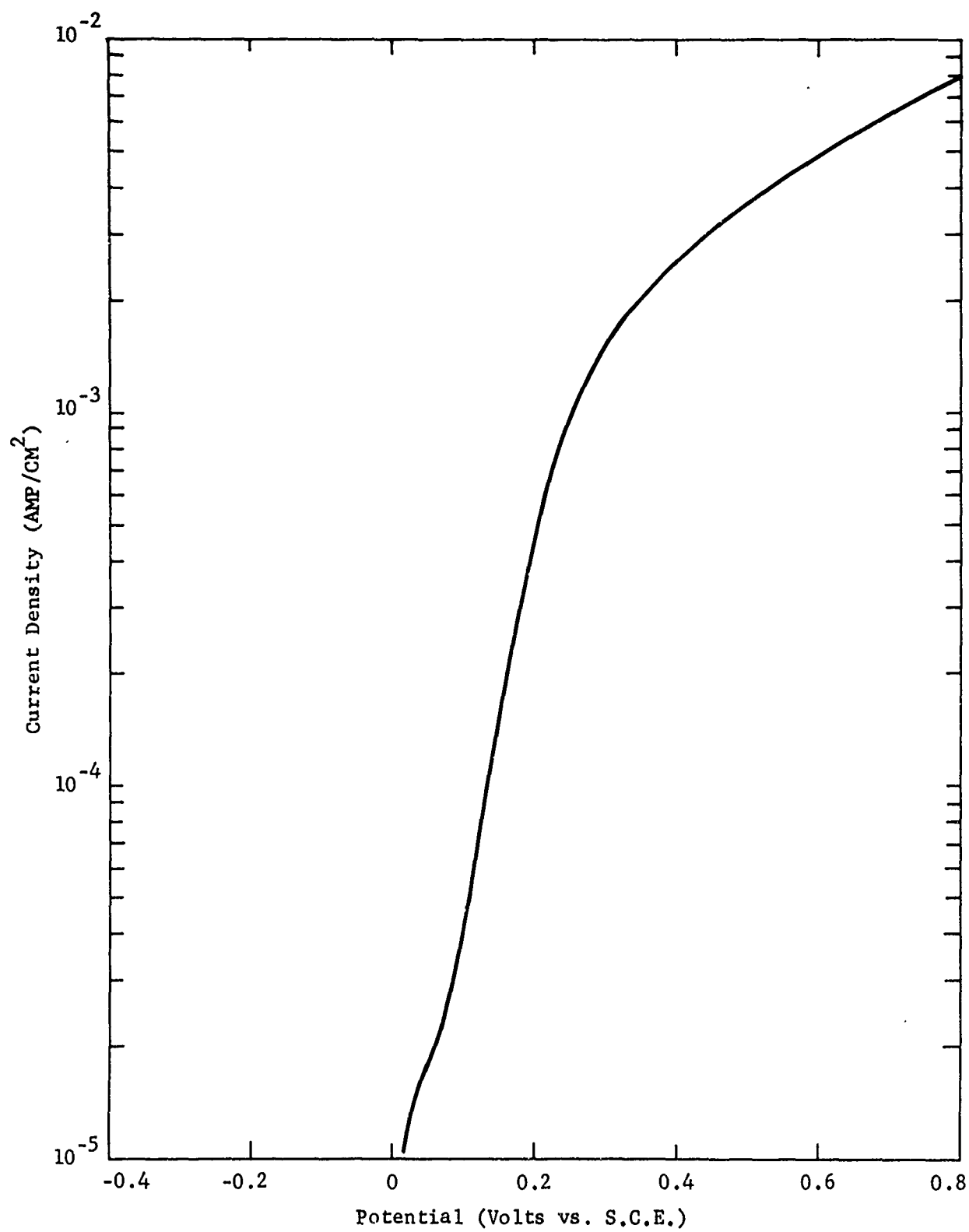


Figure 7. Anodic polarization of copper alloy 624 in air-saturated tap water at 50C.

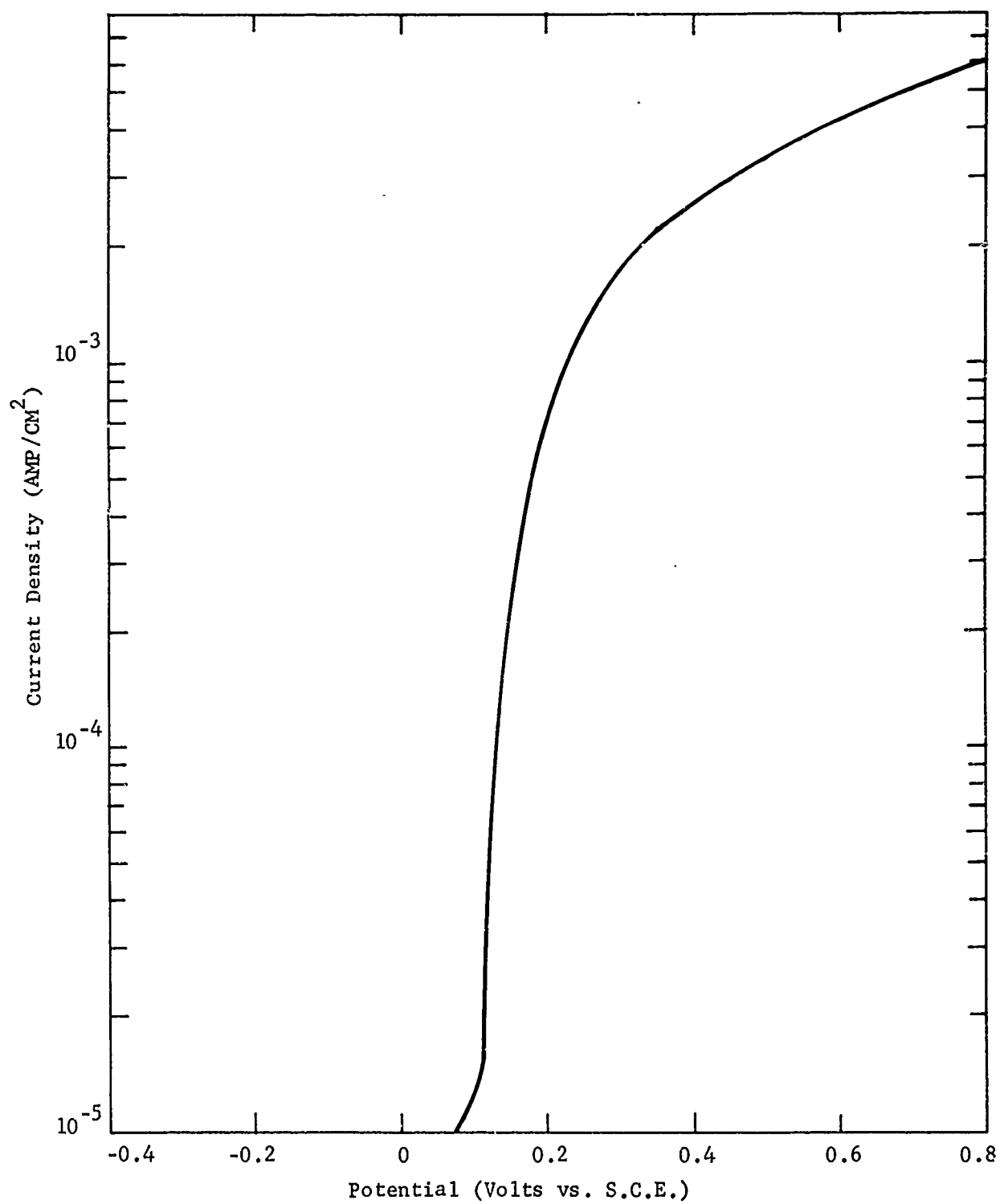


Figure 8. Anodic polarization of ASTM B140 Alloy "A" in air-saturated tap water at 25C.

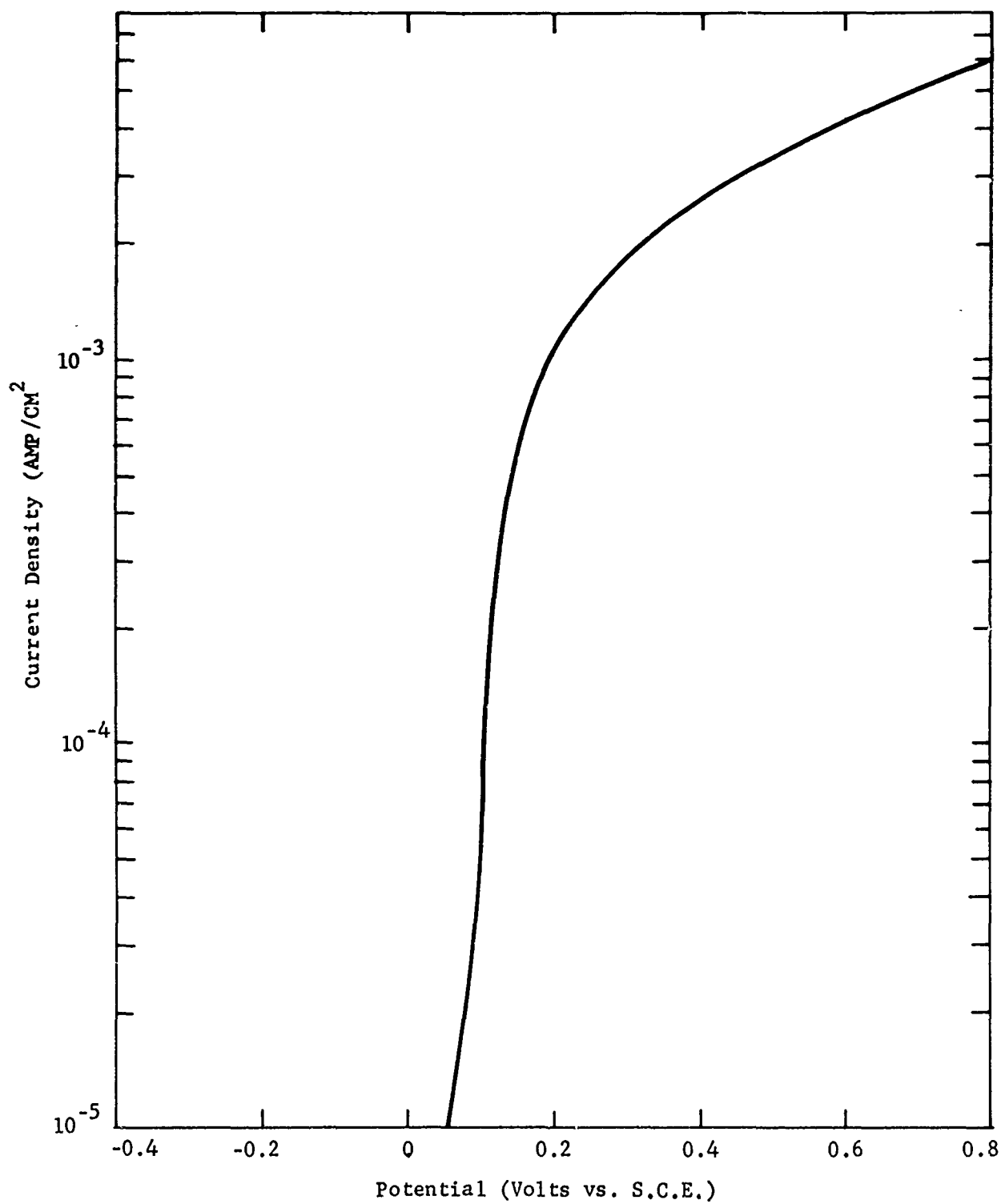


Figure 9. Anodic Polarization of ASTM B140 Alloy "A" in air-saturated tap water at 50C.

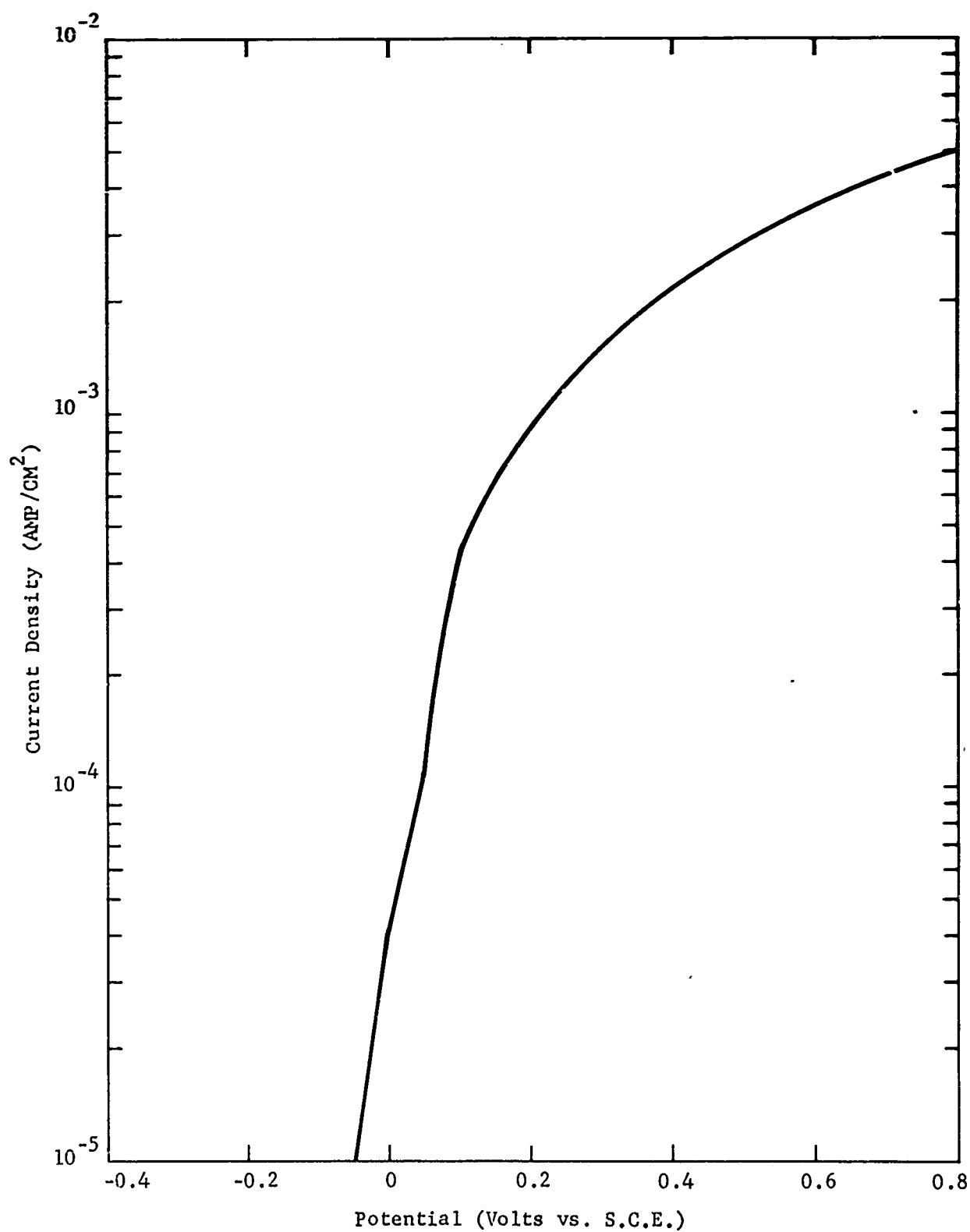


Figure 10. Anodic polarization of ASTM B62 in air-saturated tap water at 50C.



## Appendix A

### GLOSSARY OF ELECTROCHEMICAL TERMS

- $E_{\text{corr}}$  Corrosion Potential. The potential of a corroding metal with no applied current, also referred to as the open-circuit potential.
- $I_{\text{corr}}$  Corrosion Current. The current at the corrosion potential, directly proportional to the corrosion rate.
- $E_{\text{pp}}$  Primary Passive Potential. The potential of a corroding electrode where the current reaches a maximum in a potentiostatic anodic polarization.
- $I_{\text{cr}}$  Critical Current. The current at the Primary Passive Potential.

## Appendix B

### APPLICATION OF POLARIZATION CURVES TO CORROSION TESTING

Some of the important corrosion data that a maintenance engineer needs to know are: How fast a metal (or alloy) corrodes, how the corrosion rate changes with time, and which of several alloys corrodes the fastest in a particular environment. This information can often be obtained from conventional weight loss measurements; however, this is invariably a slow procedure involving exposure of specimens for long periods of time. Alternatively, the answers could be obtained rapidly from electrochemical kinetic measurements.

The basis of electrochemical corrosion is Faraday's law which relates chemical change to electric currents. In a corroding system this law may be stated as  $w/t = kI$ , where  $w$  is the weight of metal reacting,  $t$  is the time,  $I$  is the current, and  $k$  is a constant for each metal, called the electrochemical equivalent. Thus the corrosion rate is directly proportional to the current.

When a metal is immersed in an aggressive solution an oxidation reaction (dissolution of the metal) begins to take place at certain sites of the metal surface; at other sites on the surface a reduction reaction (such as the evolution of hydrogen) takes place. After a period of time a constant potential is reached indicating that corrosion is occurring at a steady rate and a "steady-state" is achieved. It should be emphasized that this steady-state is reached without any external current applied to the corroding metal and therefore is usually referred to as open-circuit or no-current steady-state. In electrochemical terminology the electrode potential of the corroding metal in the open-circuit steady-state is called the "corrosion potential" and the corresponding current is called the "corrosion current". If an external current is now applied to the corroding metal, the electrode potential is displaced from the corrosion potential; the difference between the corrosion potential and the potential resulting after current is applied is referred to as the "polarization". A polarization plot is a plot of applied current (usually expressed as current density, i.e., applied current divided by the area of the metal electrode) versus electrode potential. "Potentiostatic" polarization refers to an experimental procedure in which the electrode potential is the independent variable.

Of particular interest to the corrosion engineer is the anodic polarization plot in which the metal is polarized in the increasingly positive direction. Unless passivity is involved, the corrosion rate generally increases as the electrode potential becomes more noble. If the electrode exhibits active-passive corrosion behavior, the corrosion rate increases up to the "primary passive potential" corresponding to the maximum corrosion rate (critical anodic current density) and then decreases at more noble electrode potentials. Passivity is generally attributed to the formation of a protective film on the metal surface.

The electrochemical behavior of a system corroding under activation control, that is where both the anodic and cathodic processes making up the corrosion reaction are controlled by simple ionization, can be described by the following equations, referred to as Tafel equations:

$$E = E_{\text{corr}} - E_I$$

$$E = B_a \log I_a / I_{\text{corr}} = -B_c \log I_c / I_{\text{corr}}$$

where  $E$  = Polarization  
 $E_I$  = Polarized (Current Flowing) Potential  
 $E_{\text{corr}}$  = Corrosion Potential  
 $I_{\text{corr}}$  = Corrosion Current  
 $B_a$  and  $B_c$  = Anodic and Cathodic Tafel slopes  
 $I_a$  and  $I_c$  = Anodic and Cathodic Currents

From the above equations and the relationship

$$I_{\text{app}} \text{ (Applied Current)} = I_a - I_c$$

it can be shown that:

1. For small values of  $E$ , that is, where the polarization is about 10 mv or less,

$$\Delta E / \Delta I_{\text{app}} = B_a B_c / 2.3 I_{\text{corr}} (B_a + B_c)$$

and the corrosion rate,  $I_{\text{corr}}$ , at the corrosion potential can be obtained. If accurate values of the Tafel slopes are known, then absolute corrosion rates can be calculated; however, it is often sufficient only to determine relative corrosion rates for the purpose of screening alloys, measuring the change of corrosion rates with time, and evaluating inhibitors.

2. For large values of  $E$ , that is, where the polarization is about 50 mv or more, the applied current is essentially proportional to the corrosion rate.

The time required to obtain a polarization curve varies from a few minutes to several hours. From this moderate investment in time, the laboratory corrosion engineer can derive a profile of corrosion rates starting from the corrosion potential and extending over the whole range of potentials. In addition valuable information can be obtained regarding the mechanism of corrosion, the corrosivity of the environment, and the best method for corrosion control.

## Appendix C

### PRESENT VALUE ANALYSIS TO DETERMINE MOST ECONOMICAL TYPE OF VALVE

by

J. G. Kirby

Valve failure can be greatly accelerated when dezincification is present in the environment. Low zinc content valve stems, with resulting longer valve life, are available at an additional cost.

This appendix compares the present value of replacement costs for three types of valves listed below. Economic life spans were not available for the three valves; however, Dr. Porte felt that five years would be a good estimate for Valve #1.

<u>Valve</u>	<u>Valve Stem</u>	<u>Cost*</u>
1	ASTM B140 Alloy A <sup>2/</sup>	\$15.10
2	ASTM F99 Alloy B <sup>1/</sup>	15.90
3	ASTM B99 Alloy B <sup>1/</sup>	19.10

<sup>1/</sup>ASTM B99 Alloy B; zinc content 1.5%

<sup>2/</sup>ASTM B140 Alloy A; zinc content 11 to 15%

\* Includes labor to remove and replace (\$6.50) but not travel

Comparison calculations were then made with the assumptions that the two other valves would last 1, 2, 3, 4 or 5 years longer. The exact figure would, of course, have to be determined experimentally.

References 8 and 9 indicate that a 10% discount rate should be used in the present value calculations.

Present value analysis requires that the costs of all alternatives be compared at the same point in time and that benefits from all alternatives accrue for the same length of time. For example, if one valve lasts for five years and another for seven, a valid comparison of costs can only be made if a time period of thirty-five years is used (i.e. present value of total cost of seven of the first stem versus cost of five of the second type). The table below indicates the required time periods for the various assumptions of additional life.

Table 1. Common Time Periods.

<u>Assumed Additional Life (years)</u>	<u>Valve 1</u>	<u>Valve 2</u>	<u>Valve 3</u>	<u>Common Time Period (years)</u>
1	6 @5 yrs	5 @6 yrs	5 @6 yrs	30
2	7 @5 yrs	5 @7 yrs	5 @7 yrs	35
3	8 @5 yrs	5 @8 yrs	5 @8 yrs	40
4	9 @5 yrs	5 @9 yrs	5 @9 yrs	45
5	2 @5 yrs	1 @10 yrs	1 @10 yrs	10

For present value calculations the interest/year rate (10%) must be transformed into an interest/period rate, where the period ranges from five to ten years. This can be accomplished by means of the compound interest formula,

$$i (\text{interest/period}) = (1 + .10)^n - 1$$

where n = number of years/period

Table 2. Equivalent Interest Rate.

<u>Years/Period</u>	<u>Equivalent Interest Rate</u>
5	61.051%
6	77.156%
7	94.872%
8	114.359%
9	135.795%
10	159.374%

The cost of using the valves for the common time period can be considered as a uniform series of payments over time. The present value factor for the uniform series is given by

$$PV = 1 + \frac{(1+i)^n - 1}{i(1+i)^n}$$

where  $i$  is from Table 2 and  $n$  = number of periods - 1

Table 3. Present Value Factors.

<u>Assumed Additional Life (years)</u>	<u>Valve 1</u>	<u>Valve 2</u>	<u>Valve 3</u>	<u>Common Time Period (years)</u>
1	2.487	2.164	2.164	30
2	2.544	1.981	1.981	35
3	2.580	1.833	1.833	40
4	2.602	1.713	1.713	45
5	1.621	1.000	1.000	10

Multiplying the entries in Table 3 by the given cost figures yields the present value of the cost of each valve under the various assumptions about extended life.

Table 4. Present Value of Costs

<u>Assumed Additional Life (years)</u>	<u>Valve 1</u>	<u>Valve 2</u>	<u>Valve 3</u>	<u>Common Time Period (years)</u>
1	\$37.55	\$34.41	\$41.33	30
2	38.51	30.37	37.84	35
3	38.96	29.14	35.01	40
4	39.29	27.24	32.71	45
5	24.47	15.90	19.10	10

For clarity, the information in Table 4 was transformed into cost/year figures by the inverse of the present value factor for a uniform series. Since the desired results are in terms of cost/year, the recommended 10% discount rate was used.

Table 5. Annual Cost.

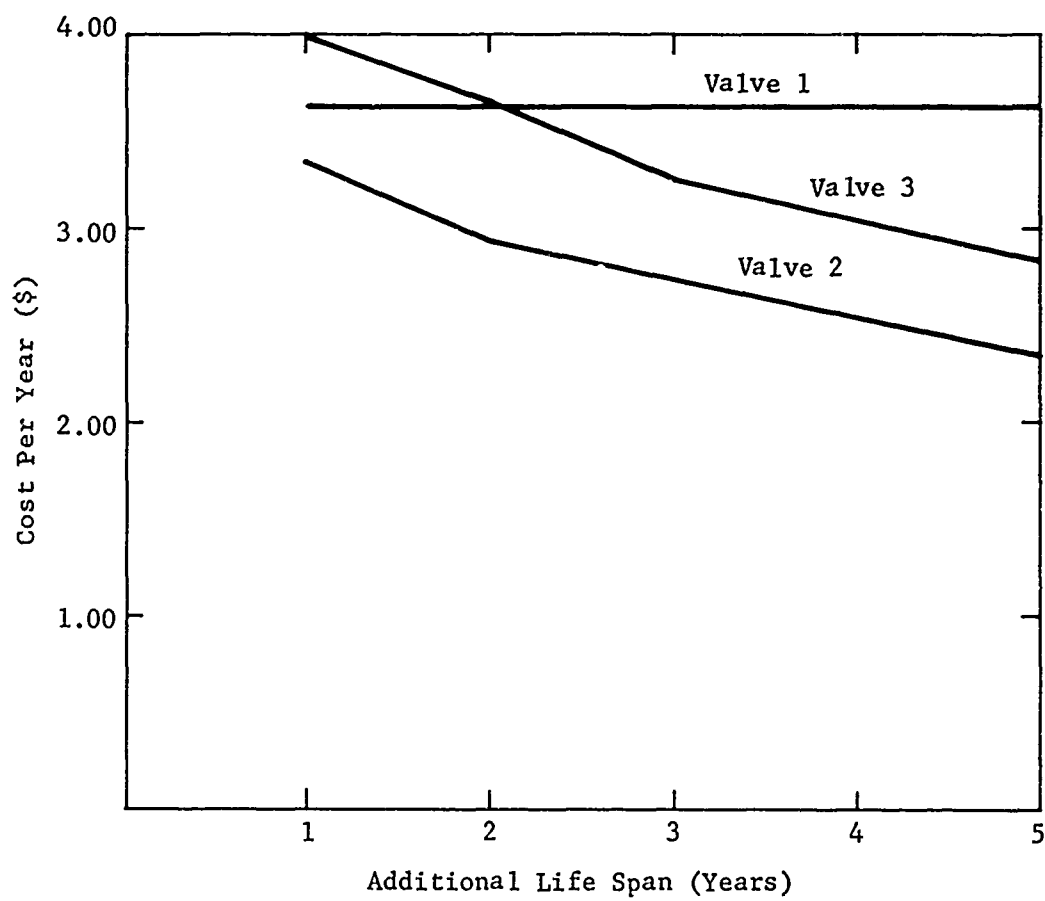
<u>Assumed Additional Life (years)</u>	<u>Valve 1</u>	<u>Valve 2</u>	<u>Valve 3</u>
1	\$3.62	\$3.32	\$3.99
2	3.62	2.93	3.65
3	3.62	2.71	3.26
4	3.62	2.51	3.02
5	3.62	2.36	2.83

For convenience, the information of Table 5 is presented in graphic form (see Graph 1). Once the number of years of extended life for Valves 2 and 3 are determined experimentally, the minimum cost policy can easily be found. This is accomplished by comparing the cost related to the extended life of Valves 2 and 3 against the corresponding cost for Valve 1. The minimum cost policy is then given by the minimum of these numbers. For example, if Valve 2 has an extended life of one year and Valve 3 four, the two pairs of numbers to compare are:

Valve 1 = \$3.63  
Valve 2 = 3.32

Valve 1 = \$3.62  
Valve 3 = 3.02

In this case, the optimum policy is thus to purchase Valve 3.



Graph C-1. Annual Cost For Valves.



#### REFERENCES

1. L. E. Tabor, "Effects of Softened Water on Equipment," in American Water Works Association, Vol. 48, 1956, pp. 239-246.
2. H. H. Uhlig, "Corrosion and Corrosion Control," John Wiley & Sons, Incorporated, New York, 1963, p. 290.
3. E. W. Palmer, "Project No. IR-31, Dezincification Study of Alloy 6941 by Potentiostatic Means," in Anaconda American Brass Company Report, 1966.
4. R. Heidersbach, "Clarification of the Mechanism of the Dealloying Phenomenon," in Corrosion, Vol. 24, 1968, pp. 38-44.
5. H. Sugawara and H. Ebiko, "Dezincification of Brass," in Corrosion Science, Vol. 7, 1967, pp. 513-523.
6. E. P. Polushkin and M. Shuldener, TAIPE, Vol. 161, 1945, p. 214.
7. C. R. Southwell, A. L. Alexander and C. W. Hummer, Jr., "Corrosion of Metals in Tropical Environments--Copper and Wrought Copper Alloys," in Materials Protection, Vol. 7, 1968, pp. 41-47.
8. NAVCOMPTINST 7000.20 of 19 April 1967.
9. "Survey of the Discounting Techniques in Evaluation Future Programs", report to Joint Economic Committee Congress of the United States by the Comptroller General of the United States, 29 January 1968.

UNCLASSIFIED

Security Classification

DOCUMENT CONTROL DATA - R & D		
Security Classification of title, body of abstract and indexing annotation must be entered when the overall report is classified		
1. ORIGINATING ACTIVITY (Corporate author) Naval Civil Engineering Laboratory Port Huensme, California		2a. REPORT SECURITY CLASSIFICATION Unclassified
		2b. GROUP
3. REPORT TITLE A Potentiostatic Dezincification Study		
4. DESCRIPTIVE NOTES (Type of report and inclusive dates) Final      October 1967 - June 1968		
5. AUTHOR(S) (First name, middle initial, last name) Howard A. Porte		
6. REPORT DATE January 1969	7a. TOTAL NO. OF PAGES 32	7b. NO. OF REFS 7
6a. CONTRACT OR GRANT NO.  b. PROJECT NO Y-F015-20-02-024  c.  d.	9a. ORIGINATOR'S REPORT NUMBER(S) Technical Note N-1005	
9b. OTHER REPORT NO(S) (Any other numbers that may be assigned this report)		
10. DISTRIBUTION STATEMENT Each transmittal of this document outside the agencies of the U. S. Government must have prior approval of the U. S. Naval Civil Engineering Laboratory.		
11. SUPPLEMENTARY NOTES		12. SPONSORING MILITARY ACTIVITY Naval Facilities Engineering Command Washington, D.C.
13. ABSTRACT <p>The objective of this study was to determine the dezincification rate of commercially available valve stems containing varying amounts of zinc. Potentiostatic anodic polarization tests were conducted on copper (electrolytic tough pitch) and four copper alloys - copper alloy 377 (forging brass), ASTM B140 Alloy "A" (lead red brass), ASTM B62 (85-5-5-5), and copper alloy 624 (aluminum bronze) - in laboratory tap water at 25C (77F) and 50C (122F) and in 0.5 molar aqueous sodium chloride (0.5M NaCl) at 25C. Dezincification was found in copper alloy 377 in laboratory tap water at 25C, corroborating field experience that high zinc content valve stems are subject to dezincification attack. Both ASTM B140 Alloy "A" and copper alloy 624 showed no visible attack at 25C in laboratory tap water but did show evidence of dealloying attack at 50C; these alloys could be expected to perform satisfactorily in cold water but are not recommended for hot water systems. ASTM B62 did not show any dezincification attack at 50C in laboratory tap water, this alloy is recommended for valve stems in both cold and hot water systems. These tests suggest that the potentiostatic method is applicable as an accelerated test for detecting susceptibility to dealloying attack in copper alloys.</p>		

DD FORM 1473 (PAGE 1)

1 NOV 65  
S/N 0101-807-6801

UNCLASSIFIED

Security Classification

UNCLASSIFIED

Security Classification

14 KEY WORDS	LINK A		LINK B		LINK C	
	ROLE	WT	ROLE	WT	ROLE	WT
Copper Copper alloys Anodic polarization Electrolysis Zinc Valves Water distribution						

UNCLASSIFIED

Security Classification